

ME 647

Assignment 3

Dhananjay Chimnani (218070333)

Contents

| | |
|---|-----------|
| 1 Coherent Structures and Flow Topology | 2 |
| 1.1 Velocity Gradient Tensor and its invariants | 2 |
| 1.2 Calculation of the velocity gradient tensor, eigenvalues, PDF plots | 3 |
| 1.3 Verifying the continuity equation | 4 |
| 1.4 Plotting the fields of Q/Q_{rms} and R/R_{rms} | 4 |
| 1.5 Flow description using Q vs R profile | 7 |
| 2 Lagrangian Aspects of Turbulence | 9 |
| 2.1 Lagrangian Trajectories for different T values for $N_p = 20$ | 9 |
| 2.1.1 T = 1 | 9 |
| 2.1.2 T = 5 | 9 |
| 2.1.3 T = 10 | 10 |
| 2.2 Trapping of Some Particles for $N_p = 1000$ | 10 |
| 2.3 Mean Square Displacement | 11 |
| 2.4 Calculation of Turbulent Diffusivity Coefficient | 12 |
| 2.5 Richardson pair dispersion | 12 |
| 2.5.1 Plotting the pair separation of trajectories | 13 |
| 2.5.2 Calculation of the Lyapunov exponent | 15 |
| 3 Note | 17 |

1 Coherent Structures and Flow Topology

1.1 Velocity Gradient Tensor and its invariants

Let the velocity gradient tensor $A_{ij} = \frac{\partial u_i}{\partial x_j}$ be represented by the following 3×3 matrix:

$$A_{ij} = \begin{bmatrix} \frac{\partial u}{\partial x} & \frac{\partial u}{\partial y} & \frac{\partial u}{\partial z} \\ \frac{\partial v}{\partial x} & \frac{\partial v}{\partial y} & \frac{\partial v}{\partial z} \\ \frac{\partial w}{\partial x} & \frac{\partial w}{\partial y} & \frac{\partial w}{\partial z} \end{bmatrix}$$

We can decompose A_{ij} into a symmetric part S_{ij} and an anti-symmetric part R_{ij} , such that:

$$A_{ij} = S_{ij} + R_{ij}$$

The symmetric part S_{ij} is given by:

$$S_{ij} = \frac{1}{2} \left(\frac{\partial u_i}{\partial x_j} + \frac{\partial u_j}{\partial x_i} \right)$$

The anti-symmetric part R_{ij} is given by:

$$R_{ij} = \frac{1}{2} \left(\frac{\partial u_i}{\partial x_j} - \frac{\partial u_j}{\partial x_i} \right)$$

$$A - \lambda I = \begin{bmatrix} A_{11} - \lambda & A_{12} & A_{13} \\ A_{21} & A_{22} - \lambda & A_{23} \\ A_{31} & A_{32} & A_{33} - \lambda \end{bmatrix}$$

$$\det(A - \lambda I) = \begin{vmatrix} A_{11} - \lambda & A_{12} & A_{13} \\ A_{21} & A_{22} - \lambda & A_{23} \\ A_{31} & A_{32} & A_{33} - \lambda \end{vmatrix}$$

$$(A_{11} - \lambda) \begin{vmatrix} A_{22} - \lambda & A_{23} \\ A_{32} & A_{33} - \lambda \end{vmatrix} - A_{12} \begin{vmatrix} A_{21} & A_{23} \\ A_{31} & A_{33} - \lambda \end{vmatrix} + A_{13} \begin{vmatrix} A_{21} & A_{22} - \lambda \\ A_{31} & A_{32} \end{vmatrix} = 0$$

$$(A_{11} - \lambda)[(A_{22} - \lambda)(A_{33} - \lambda) - A_{23}A_{32}] - A_{12}[A_{21}(A_{33} - \lambda) - A_{23}A_{31}] + A_{13}[A_{21}A_{32} - (A_{22} - \lambda)A_{31}] = 0$$

After expanding and simplifying, this leads to the characteristic polynomial:

$$\lambda^3 + P\lambda^2 + Q\lambda + R = 0$$

$$P = -(A_{11} + A_{22} + A_{33})$$

$$Q = A_{11}A_{22} + A_{22}A_{33} + A_{11}A_{33} - A_{13}A_{31} - A_{12}A_{21} - A_{23}A_{32}$$

$$R = -\det(A)$$

From the properties of cubic equations:

$$\lambda_1 + \lambda_2 + \lambda_3 = -P$$

$$\lambda_1\lambda_2 + \lambda_2\lambda_3 + \lambda_3\lambda_1 = Q$$

$$\lambda_1\lambda_2\lambda_3 = -R$$

$$\Rightarrow \boxed{\lambda_1 + \lambda_2 + \lambda_3 = 0}$$

$$\lambda_1\lambda_2 + \lambda_2\lambda_3 + \lambda_3\lambda_1 = A_{11}A_{22} + A_{22}A_{33} + A_{11}A_{33} - A_{13}A_{31} - A_{12}A_{21} - A_{23}A_{32}$$

$$\lambda_1\lambda_2 + \lambda_2\lambda_3 + \lambda_3\lambda_1 = \frac{1}{2}((A_{11} + A_{22} + A_{33})^2 - (A_{11}^2 + A_{22}^2 + A_{33}^2)) - A_{13}A_{31} - A_{12}A_{21} - A_{23}A_{32}$$

Using an easy rearrangement of terms we get:

$$\begin{aligned} \lambda_1\lambda_2 + \lambda_2\lambda_3 + \lambda_3\lambda_1 &= \frac{1}{2}((A_{11} + A_{22} + A_{33})^2 - (A_{11}^2 + A_{22}^2 + A_{33}^2)) - \frac{1}{4}((A_{13} + A_{31})^2 - (A_{13} - A_{31})^2) \\ &\quad - \frac{1}{4}((A_{12} + A_{21})^2 - (A_{12} - A_{21})^2) - \frac{1}{4}((A_{23} + A_{32})^2 - (A_{23} - A_{32})^2) \\ \Rightarrow \lambda_1\lambda_2 + \lambda_2\lambda_3 + \lambda_3\lambda_1 &= -\frac{1}{2}(S_{11}^2 + S_{22}^2 + S_{33}^2) - (S_{13}S_{31} + R_{13}R_{31}) - (S_{12}S_{21} + R_{12}R_{21}) - (S_{23}S_{32} + R_{23}R_{32}) \\ \Rightarrow \lambda_1\lambda_2 + \lambda_2\lambda_3 + \lambda_3\lambda_1 &= -\frac{1}{2}(S_{11}^2 + S_{22}^2 + S_{33}^2 + 2S_{13}S_{31} + 2S_{12}S_{21} + 2S_{23}S_{32} + 2R_{13}R_{31} + 2R_{12}R_{21} + 2R_{23}R_{32}) \\ \Rightarrow \boxed{\lambda_1\lambda_2 + \lambda_2\lambda_3 + \lambda_3\lambda_1 = -\frac{1}{2}(S_{ij}S_{ji} + R_{ij}R_{ji})} \end{aligned}$$

Using the matrix equation analogous to our characteristic equation:

$$\begin{aligned} A^3 + PA^2 + QA + RI &= 0 \\ \Rightarrow R \cdot \text{tr}(I) &= -\text{tr}(A^3) - Q \cdot \text{tr}(A) - P \cdot \text{tr}(A^2) \\ \Rightarrow 3R &= -\text{tr}(A^3) \\ \Rightarrow \lambda_1\lambda_2\lambda_3 &= \frac{1}{3}\text{tr}(A^3) = \frac{1}{3}(A_{ij}A_{jk}A_{ki}) \\ \Rightarrow \lambda_1\lambda_2\lambda_3 &= \frac{1}{3}(S_{ij} + R_{ij})(S_{jk} + R_{jk})(S_{ki} + R_{ki}) \end{aligned}$$

Using the property that the product of a symmetric and a skew symmetric matrix gives null matrix, we get:

$$\Rightarrow \boxed{\lambda_1\lambda_2\lambda_3 = \frac{1}{3}(S_{ij}S_{jk}S_{ki} + R_{ij}R_{jk}R_{ki})}$$

1.2 Calculation of the velocity gradient tensor, eigenvalues, PDF plots

$$A_{ij} = \begin{bmatrix} \frac{\partial u}{\partial x} & \frac{\partial u}{\partial y} & \frac{\partial u}{\partial z} \\ \frac{\partial v}{\partial x} & \frac{\partial v}{\partial y} & \frac{\partial v}{\partial z} \\ \frac{\partial w}{\partial x} & \frac{\partial w}{\partial y} & \frac{\partial w}{\partial z} \end{bmatrix}$$

We calculate this velocity gradient tensor at every point of the middle z plane and then calculate the eigenvalues for each of these tensors. Subsequently, we plot the PDF of these eigenvalues. The gradients have been approximated using the central differencing scheme of the Finite Difference Method. Also, as the domain is periodic central differencing can be applied even at the boundary points. As a large part (almost one - third) of the eigenvalues are complex, we cannot directly plot a PDF. Therefore, we will make a PDF of their magnitudes.

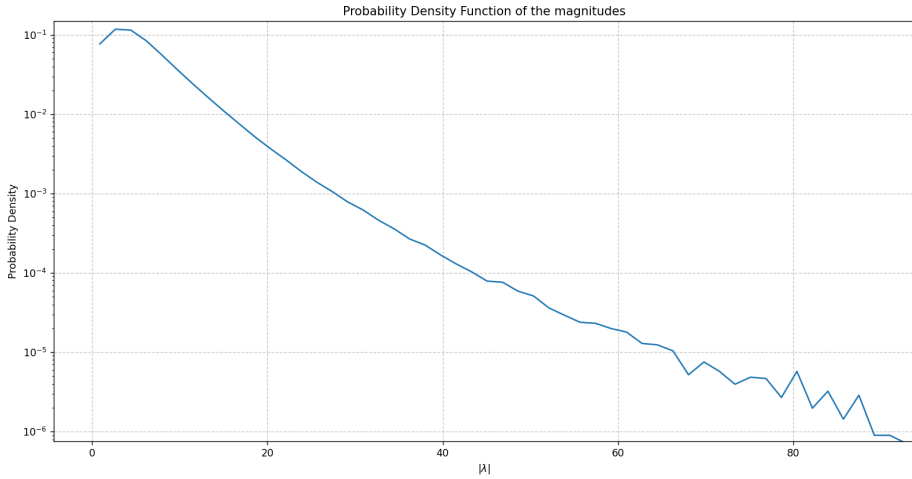
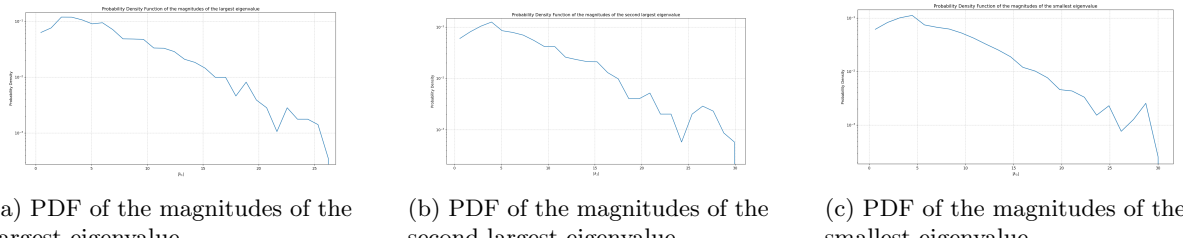


Figure 1: PDF of magnitudes of all the eigenvalues taken together (Semilog plot)



(a) PDF of the magnitudes of the largest eigenvalue

(b) PDF of the magnitudes of the second largest eigenvalue

(c) PDF of the magnitudes of the smallest eigenvalue

Figure 2: Probability density Functions of the eigenvalue magnitudes (Semilog plots)

1.3 Verifying the continuity equation

$$P = -\left(\frac{\partial u}{\partial x} + \frac{\partial v}{\partial y} + \frac{\partial w}{\partial z}\right) = 0$$

We calculate the derivatives using the central differencing scheme of the Finite difference method. Then we average the absolute value of P over all the points present in the middle z - plane. We get:

$$\langle |P| \rangle \approx 0.337$$

This is a very strange result as I expected it to come very small but the value is significantly large.

1.4 Plotting the fields of Q/Q_{rms} and R/R_{rms}

$$Q = \lambda_1 \lambda_2 + \lambda_2 \lambda_3 + \lambda_3 \lambda_1$$

$$R = -\lambda_1 \lambda_2 \lambda_3$$

Using the eigenvalues evaluated in the previous parts, we calculate the normalized fields of Q and R. For calculating this, I ignored all the values with very large magnitudes and very small magnitudes. The range of the normalized Q and R was taken to be $[-1, 1]$ as almost 95 percent values lied in this range.

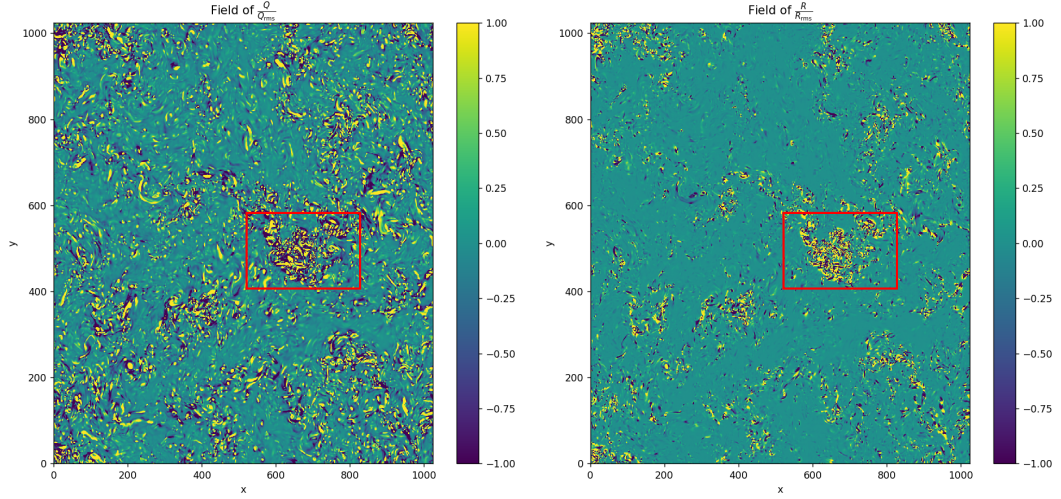


Figure 3: Complete Field of normalized second and third invariants of the velocity gradient tensor: Q/Q_{rms} and R/R_{rms} , with highlighted regions.

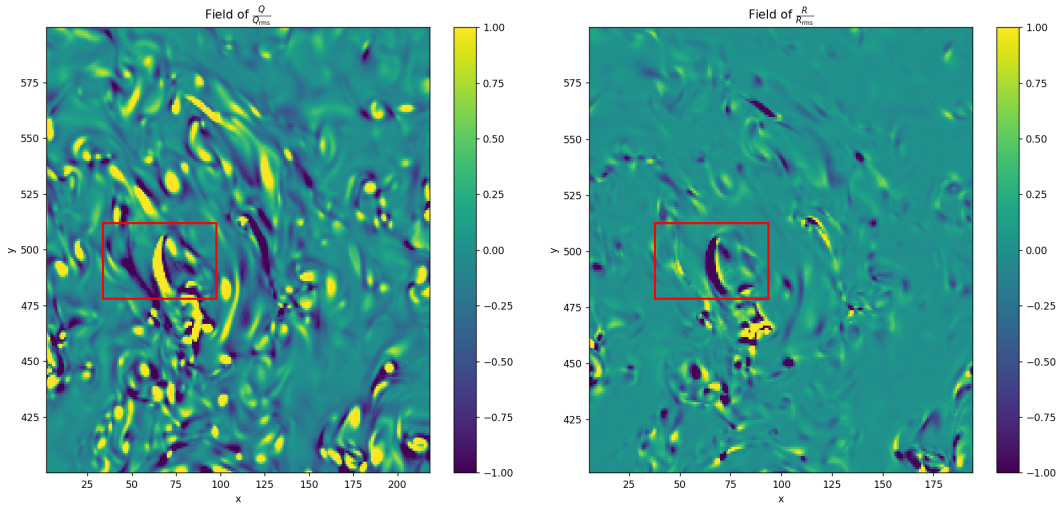


Figure 4: Field of normalized second and third invariants of the velocity gradient tensor: Q/Q_{rms} and R/R_{rms} , with highlighted regions (Zoomed view of a section).

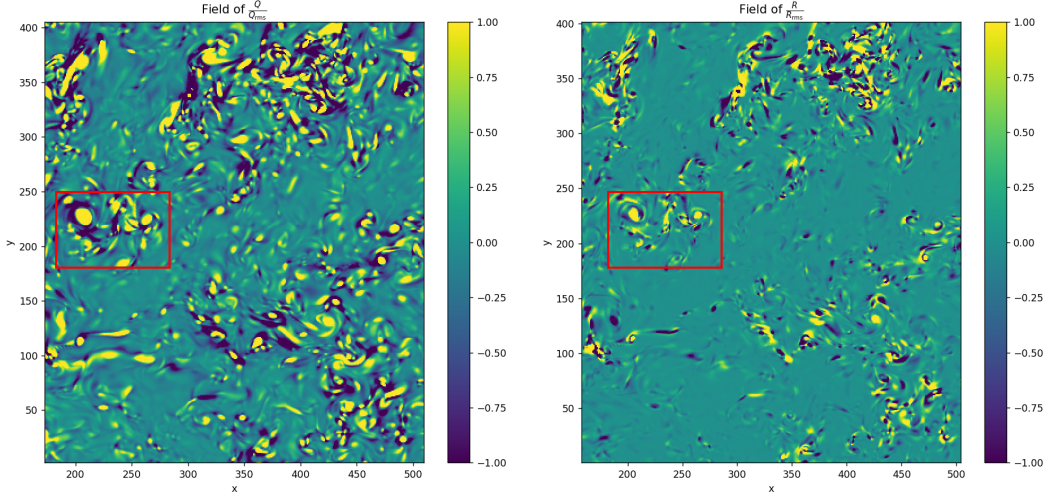


Figure 5: Field of normalized second and third invariants of the velocity gradient tensor: Q/Q_{rms} and R/R_{rms} , with highlighted regions (Zoomed view of a section).

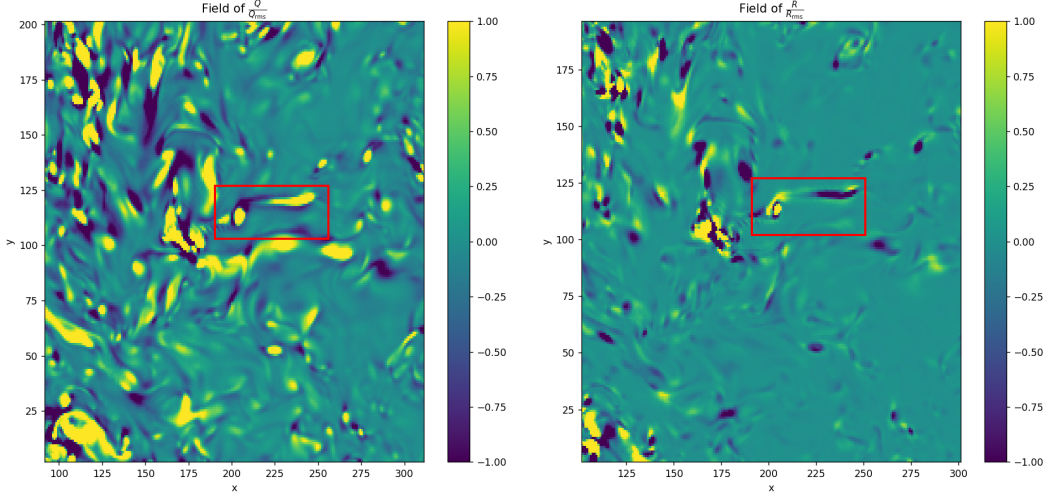


Figure 6: Field of normalized second and third invariants of the velocity gradient tensor: Q/Q_{rms} and R/R_{rms} , with highlighted regions (Zoomed view of a section).

The red boxes in the above images show that very similar structures exist in both the fields of Q and R . In Figure 3, we notice that in the red box, both Q and R have the same structural organization. Moreover, the magnitudes of both Q and R are high in the same regions and also they have the same sign. Same can be observed in Figure 5.

In Figure 4, even though we see similar structures and magnitudes, the signs are opposite. The same can be observed in Figure 6.

1.5 Flow description using Q vs R profile

In this section we plot a curve between $\frac{Q}{\langle Q_w \rangle}$ and $\frac{R}{\langle Q_w \rangle^{3/2}}$, where $\langle Q_w \rangle = \langle \omega^2 \rangle / 4$, which is known as entrosophy.

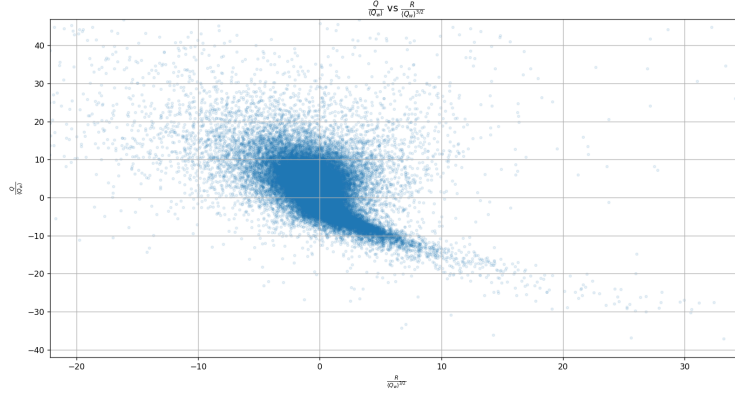


Figure 7: Tear drop shaped Q vs R profile

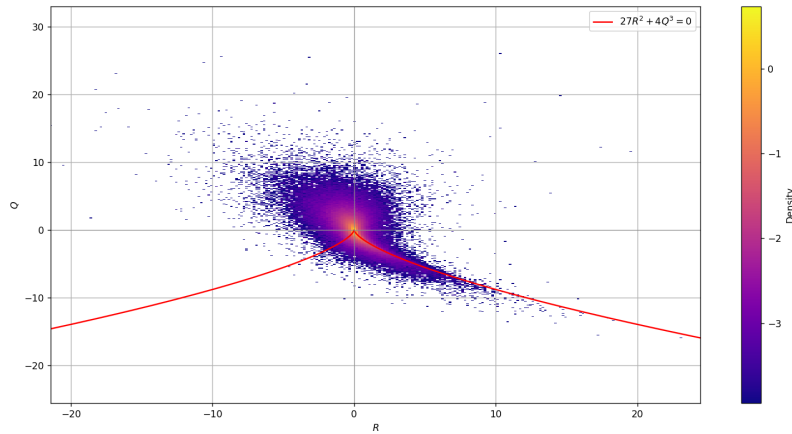


Figure 8: Joint Probability Distribution of the Q - R profile (Density is in the log scale)

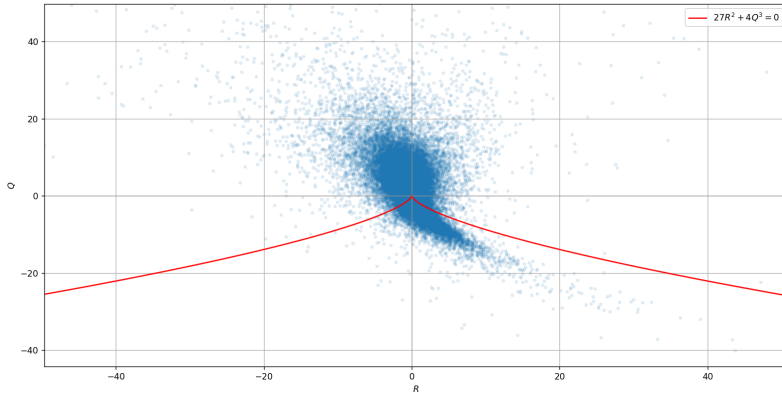


Figure 9: Q-R scatter profile with the D = 0 curve

$$D = 27R^2 + 4Q^3$$

Using the sign of D and the sign of R we can identify the prominent topologies in the flow. To identify the different topologies, the following reference plot can be used:

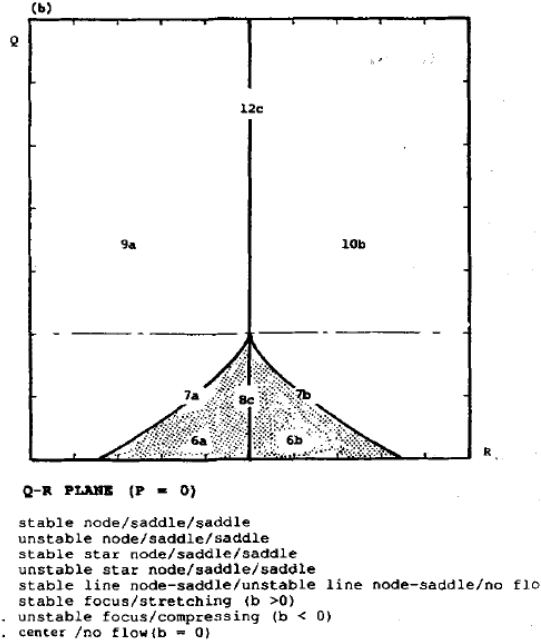


Figure 10: Image taken from 1991-Chong-Perry-Cantwell-Classification of flow fields for $P = 0$ case

For example, if at a grid point $R > 0$ and $D > 0$, it will lie in the unstable focus-compresssing zone represented by 10(b) in the Figure 10. Now, if $R < 0$ and $D < 0$, it will lie in the stable node-saddle-saddle zone represented by 6(a) in the same figure. This way I calculated the number of points lying in all the zones. The two zones with the maximum number of points in them will represent the two prominent topologies in the flow.

| Topology code | Topology | No. of points in this region |
|---------------|---|------------------------------|
| 6(a) | stable node/saddle/saddle | 94821 |
| 6(b) | unstable node/saddle/saddle | 313385 |
| 7(a) | stable star node/saddle/saddle | 0 |
| 7(b) | unstable star node/saddle/saddle | 0 |
| 8(c) | stable line node-saddle/unstable line node-saddle/no flow | 0 |
| 9(a) | stable focus/stretching | 383792 |
| 10(b) | unstable focus/compressing | 256578 |
| 12(c) | center /no flow | 0 |

This shows that **Unstable node-saddle-saddle** and **Stable focus-streching** are the prominent topologies in this flow.

Entrosphy equation derived in the assignment - 1:

$$\boxed{\frac{D\omega}{Dt} = \omega \cdot \nabla u + \nu \Delta \omega}$$

The first term on the RHS is responsible for vortex stretching or compression. Vortex stretching refers to the elongation of vortical structures in three-dimensional, incompressible flows which is caused by conservation of angular momentum. In this process, when a fluid element is stretched due to the velocity gradients, it starts spinning at a faster rate. This increase in the angular velocity is due to the conservation of the angular momentum.

2 Lagrangian Aspects of Turbulence

2.1 Lagrangian Trajectories for different T values for $N_p = 20$

2.1.1 $T = 1$

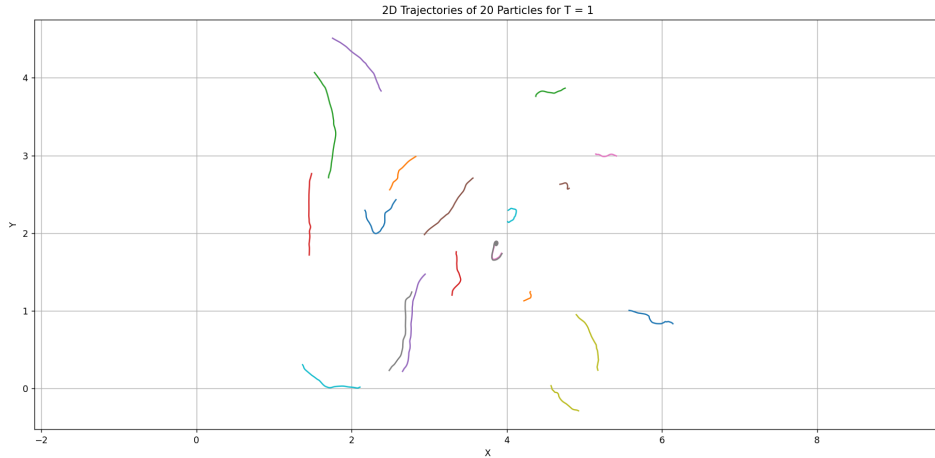


Figure 11: Lagrangian Trajectories for $T = 1$

2.1.2 $T = 5$

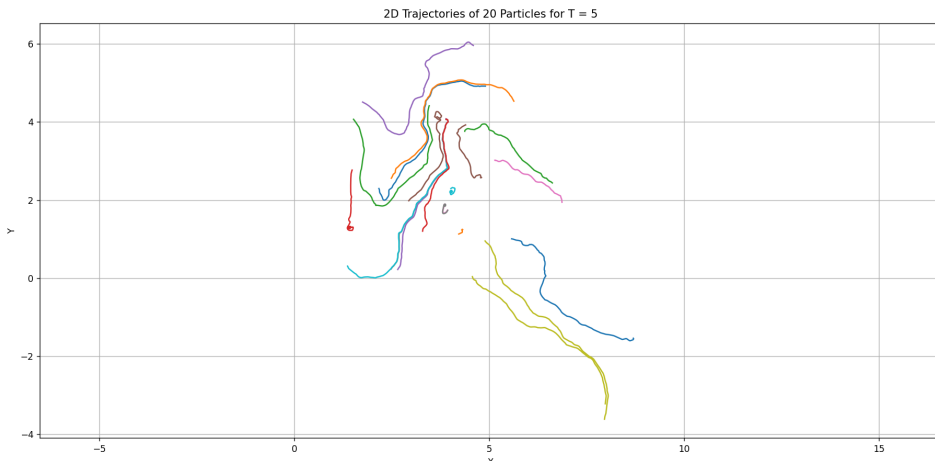


Figure 12: Lagrangian Trajectories for $T = 5$

2.1.3 $T = 10$

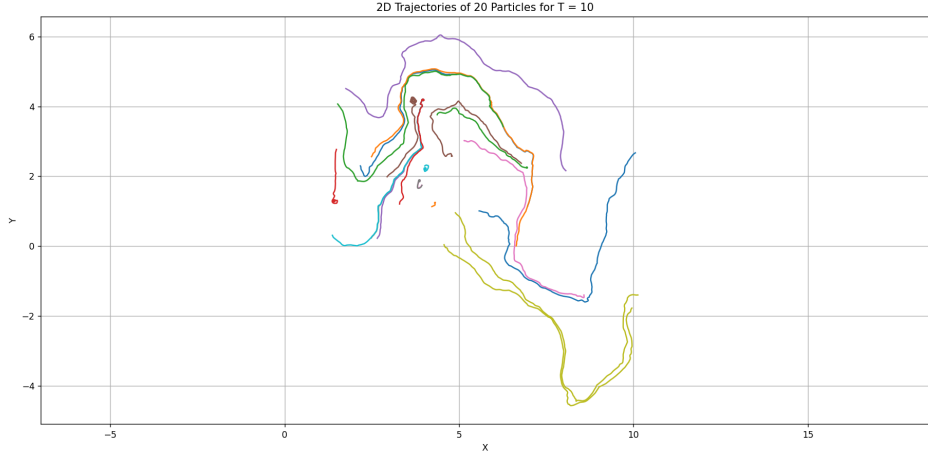
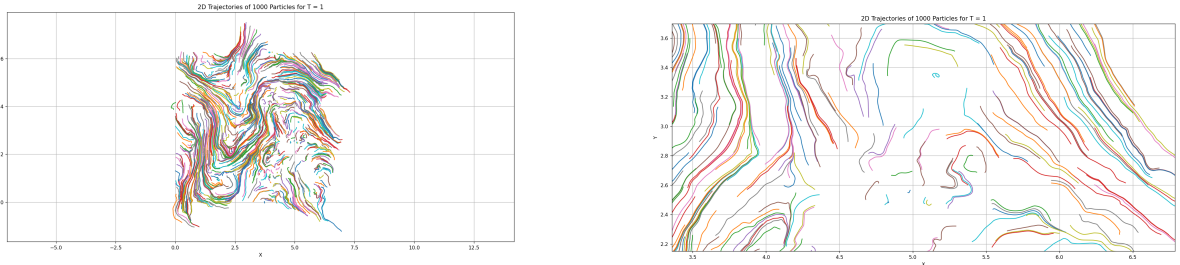


Figure 13: Lagrangian Trajectories for $T = 10$

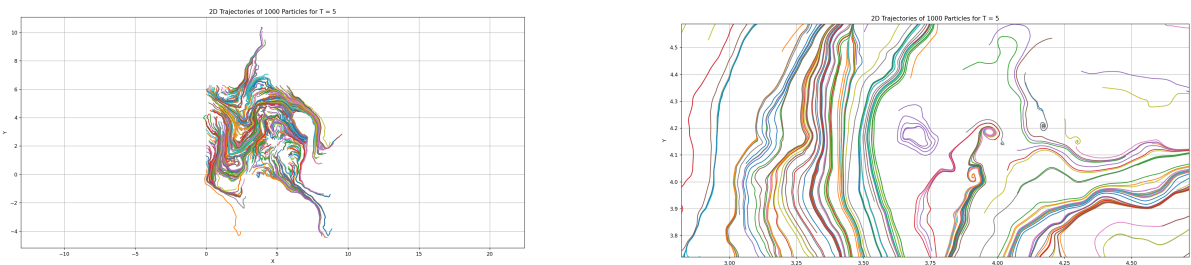
2.2 Trapping of Some Particles for $N_p = 1000$



(a) Lagrangian Trajectories for $T = 1$ for $N_p = 1000$

A zoomed section of the left image showing a trapped particle

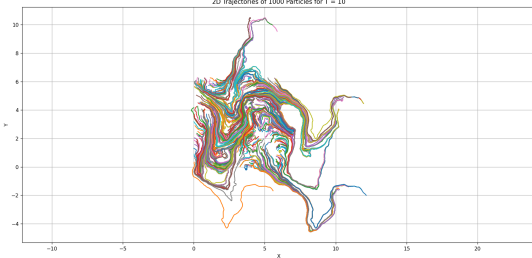
Figure 14: Trapping of Particles at $T = 1$



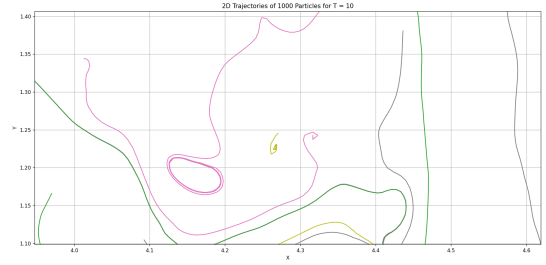
(a) Lagrangian Trajectories for $T = 5$ for $N_p = 1000$

A zoomed section of the left image showing a trapped particle

Figure 15: Trapping of Particles at $T = 5$



(a) Lagrangian Trajectories for $T = 10$ for $N_p = 1000$



A zoomed section of the left image showing a trapped particle

Figure 16: Trapping of Particles at $T = 10$

2.3 Mean Square Displacement

$$\langle \Delta r^2(t) \rangle = \langle [x(t) - x(0)]^2 + [y(t) - y(0)]^2 \rangle$$

In the ballistic regime,

$$\langle \Delta r^2(t) \rangle \sim t^2$$

$$\langle \Delta r^2(t) \rangle \sim 2\log(t) \Rightarrow \text{slope} \sim 2$$

In the diffusive regime,

$$\langle \Delta r^2(t) \rangle \sim t$$

$$\log(\langle \Delta r^2(t) \rangle) \sim \log(t) \Rightarrow \text{slope} \sim 1$$

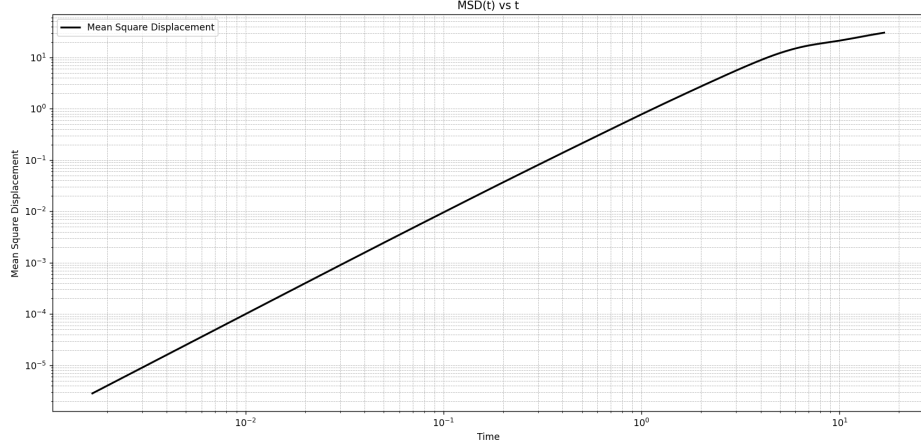


Figure 17: Mean Square Displacement vs Time (Log-Log plot)

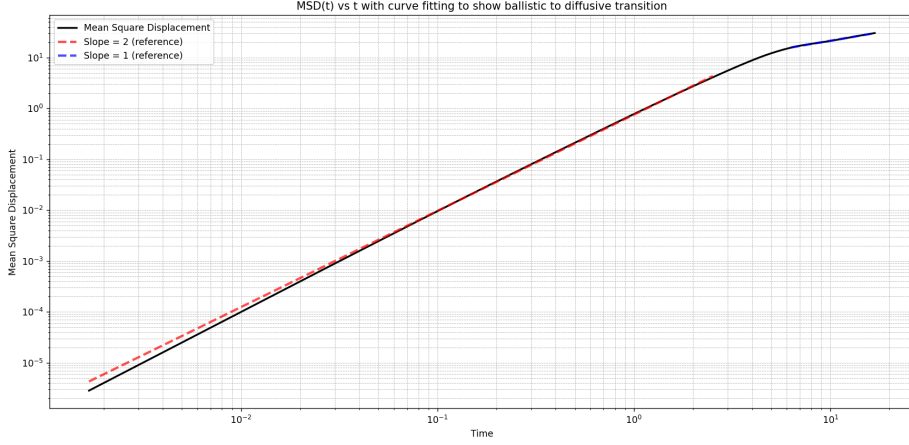


Figure 18: Capturing the transition from ballistic to diffusive regime (Log-Log plot)

The blue line completely coincides with the MSD curve in the diffusive regime, while there is a very small deviation in the red line from the MSD plot in the ballistic regime.

2.4 Calculation of Turbulent Diffusivity Coefficient

In the diffusive regime:

$$\langle \Delta r^2(t) \rangle = Dt$$

where D is the turbulent diffusivity coefficient

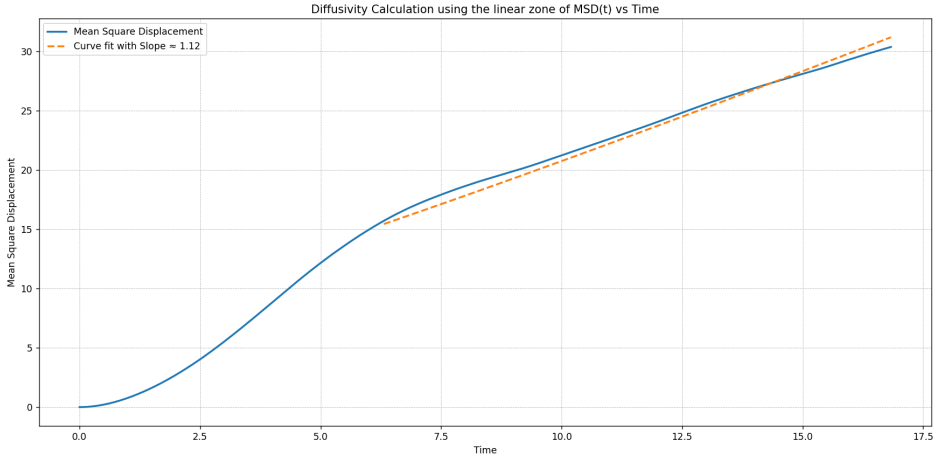


Figure 19: Turbulent Diffusivity Coefficient calculation using curve fitting in the diffusive regime

Using the slope from the above plot, we get the turbulent diffusivity coefficient as 1.12. We know that the molecular diffusivity coefficient of a dye in water is of the order 10^{-10} . Therefore, the ratio of the two quantities gives 1.2×10^{10} . Thus, the turbulent diffusivity is much higher compared to the molecular diffusivity. Therefore, in the case of turbulent flows, we can neglect the molecular diffusivity. The plot in Figure 19 is not a log-log plot.

2.5 Richardson pair dispersion

$$\Delta r^2(t) = \left\langle |\mathbf{x}_{A,i}(t) - \mathbf{x}_{B,i}(t)|^2 \right\rangle_{N_p}$$

where,

$$\mathbf{x}_{B,i}(t) - \mathbf{x}_{A,i}(t) = \epsilon$$

where, ϵ is a 2-dimensional perturbation with a fixed magnitude but random directions.

Plotting the pair trajectories

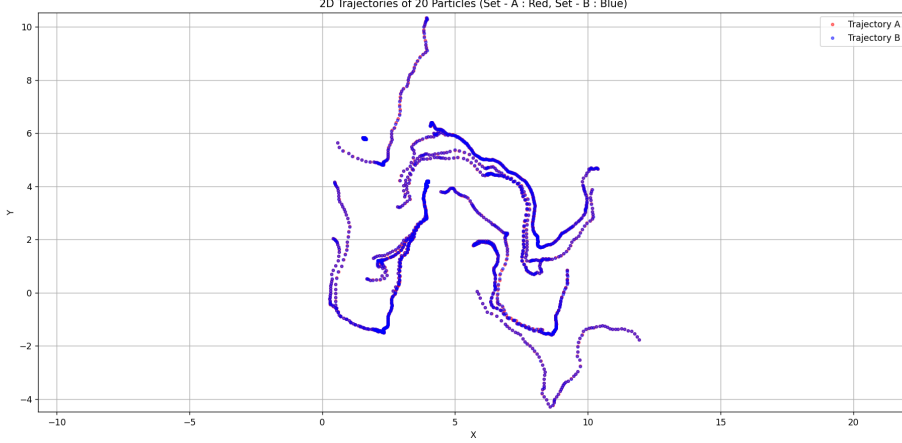


Figure 20: Pair Trajectories for $N_p = 20$, $\epsilon = 0.5 \Delta x$, $T = 10$

2.5.1 Plotting the pair separation of trajectories

In the inertial range:

$$\left\langle |\mathbf{x}_{A,i}(t) - \mathbf{x}_{B,i}(t)|^2 \right\rangle_{N_p} \sim t^\alpha$$

$$\log(\left\langle |\mathbf{x}_{A,i}(t) - \mathbf{x}_{B,i}(t)|^2 \right\rangle_{N_p}) \sim \alpha \log(t)$$

Therefore, the slope of a log-log plot will give us a straight line with slope α .

$$\epsilon = 0.1 \Delta x$$

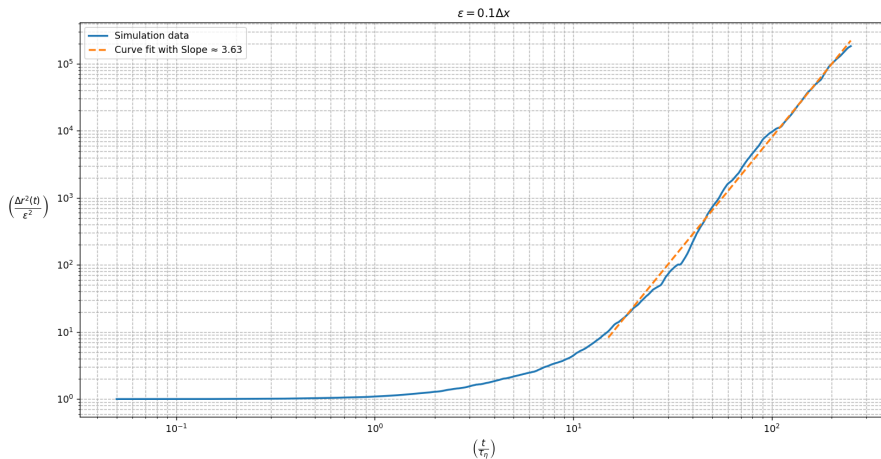


Figure 21: Pair Trajectories for $N_p = 2000$, $\epsilon = 0.1 \Delta x$, $T = 20$

$$\epsilon = 0.5 \Delta x$$

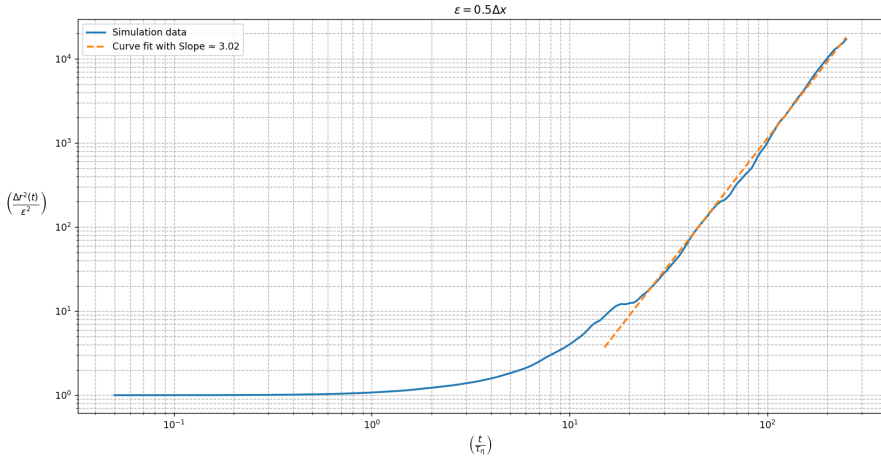


Figure 22: Pair Trajectories for $N_p = 2000$, $\epsilon = 0.5 \Delta x$, $T = 20$

$$\epsilon = 1.0 \Delta x$$

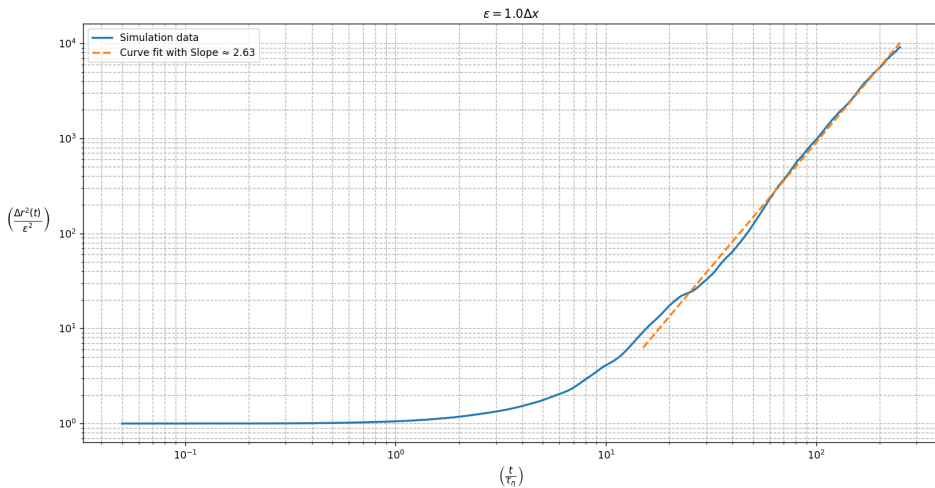


Figure 23: Pair Trajectories for $N_p = 2000$, $\epsilon = 1.0 \Delta x$, $T = 20$

$$\epsilon = 5.0 \Delta x$$

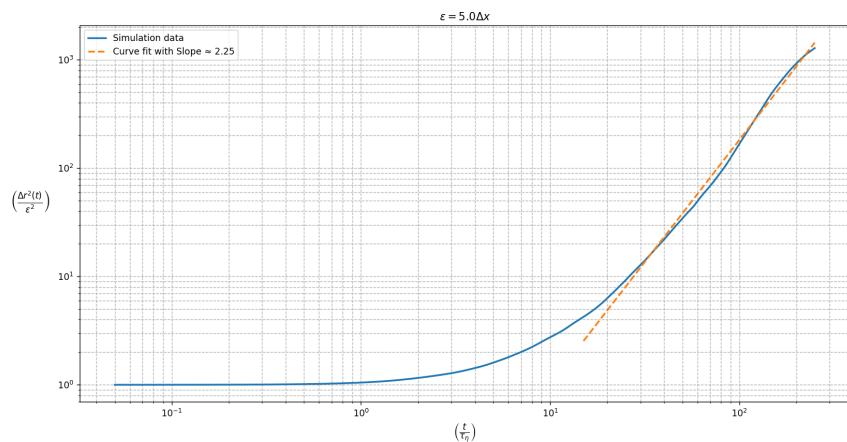


Figure 24: Pair Trajectories for $N_p = 2000$, $\epsilon = 5.0 \Delta x$, $T = 20$

$$\epsilon = 10.0 \Delta x$$

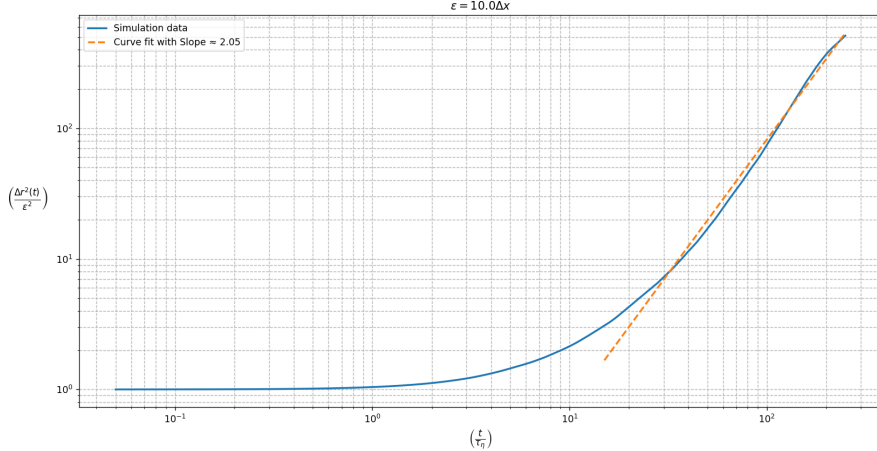


Figure 25: Pair Trajectories for $N_p = 2000$, $\epsilon = 10.0 \Delta x$, $T = 20$

The value of α lies in the range 2 - 3.5. I think if we select more random perturbations we might get alpha near 3. For calculation, I used 4 different types of perturbations. I splitted the points into 4 sections. Then gave one section a perturbation in positive x, one in the negative x, one in positive y and one in negative y. Also when I increased the total number of points, the slopes did not show any notable change.

2.5.2 Calculation of the Lyapunov exponent

If we make a semilog plot, in the initial part of the curve we see a linear trend.

$$\langle \Delta r^2(t) \rangle_{N_p} \sim e^{\Lambda t}$$

$$\Rightarrow \log(\langle \Delta r^2(t) \rangle_{N_p}) \sim (\log e) \ln(e^{\Lambda t})$$

$$\Rightarrow \log(\langle \Delta r^2(t) \rangle_{N_p}) \sim 0.434(\Lambda t)$$

$$\text{slope} = 0.434 * \Lambda \Rightarrow \boxed{\Lambda = \text{slope}/0.434}$$

$$\epsilon = 0.1 \Delta x$$

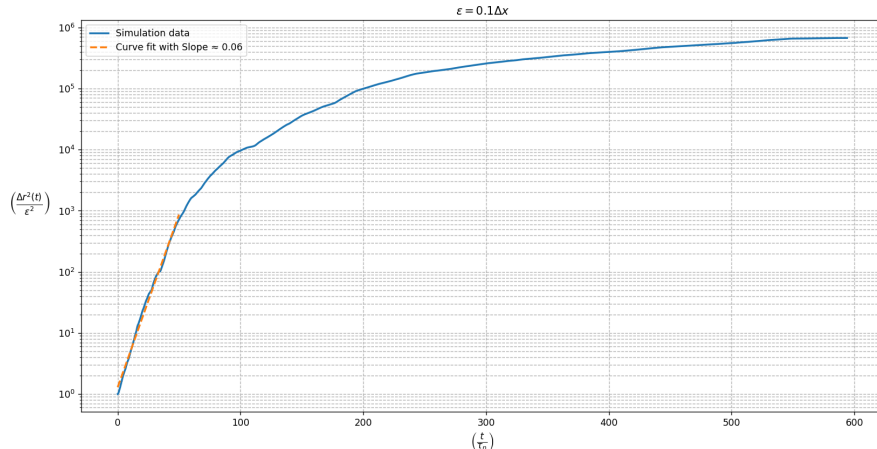


Figure 26: Pair Trajectories for $N_p = 2000$, $\epsilon = 0.1 \Delta x$, $T = 20$

$$\epsilon = 0.5 \Delta x$$

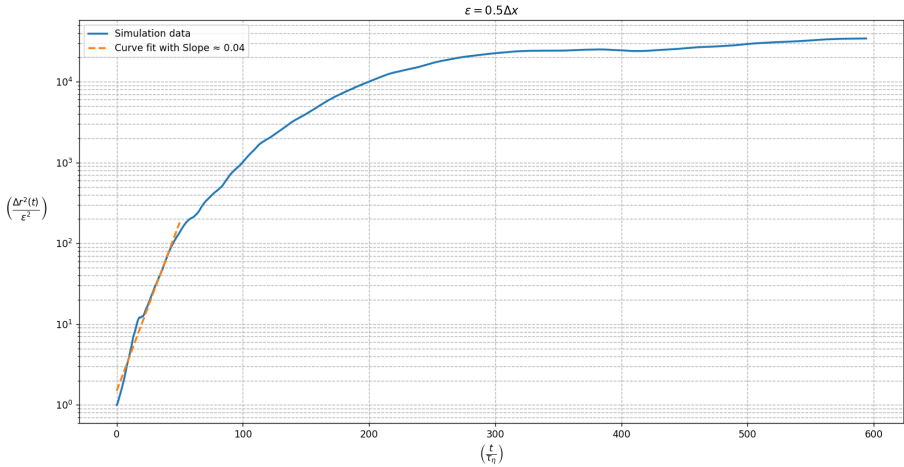


Figure 27: Pair Trajectories for $N_p = 2000$, $\epsilon = 0.5 \Delta x$, $T = 20$

$$\epsilon = 1.0 \Delta x$$

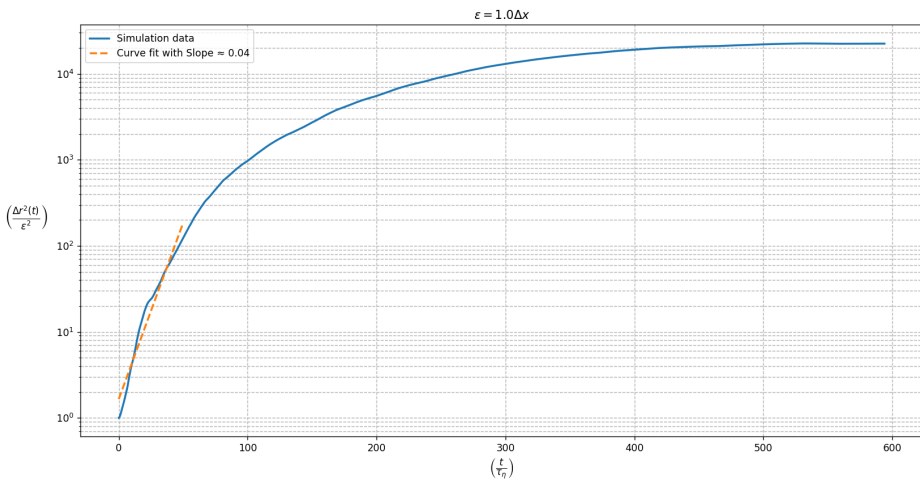


Figure 28: Pair Trajectories for $N_p = 2000$, $\epsilon = 1.0 \Delta x$, $T = 20$

$$\epsilon = 5.0 \Delta x$$

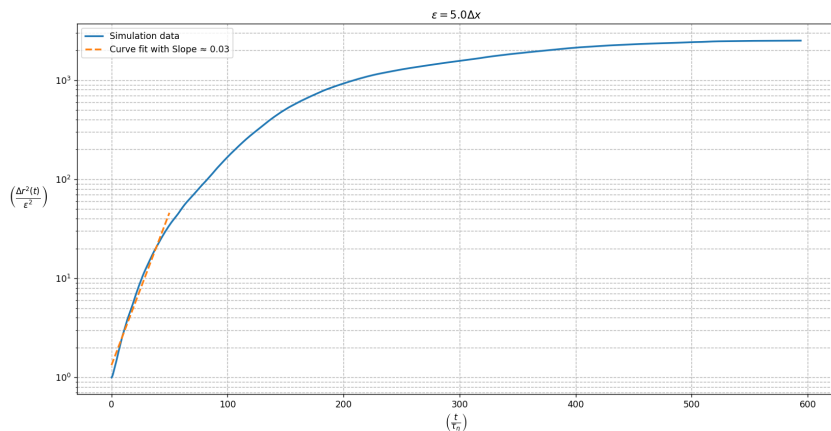


Figure 29: Pair Trajectories for $N_p = 2000$, $\epsilon = 5.0 \Delta x$, $T = 20$

$$\epsilon = 10.0 \Delta x$$

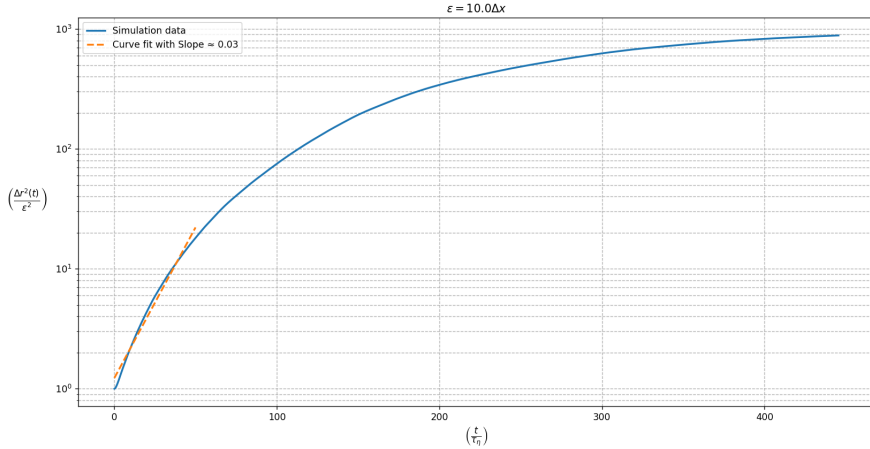


Figure 30: Pair Trajectories for $N_p = 2000$, $\epsilon = 10.0 \Delta x$, $T = 20$

Using the above trajectory plots, we observe that the slopes lies in the range 0.03 - 0.06. Therfore, using the relation derived above:

$$\Lambda = \text{slope}/0.434 \Rightarrow \boxed{\Lambda = 0.07 - 0.14}$$

3 Note

I have used ChatGPT only to write snippets for plotting, as I didn't know how to plot joint distributions, scatter plots, etc. All the logic-based code has been written by me. I also used ChatGPT for formatting my LaTeX file.